Potential Drops Supported by Ion-Density Cavities in the Dynamic Response of a Plasma Diode to an Applied Field

M. Bohm and S. Torvén

Department of Plasma Physics, Royal Institute of Technology, S-100 44 Stockholm, Sweden

(Received 9 July 1990)

A new analytical model and numerical simulations are used to show that an ion-density cavity can support large potential drops, extended over a distance related to the cavity width, for several electron transit times. When the applied potential drop exceeds a critical value, which depends on the cavity depth, the drop is instead concentrated in a cathode sheath. The existence regions for the two different states in the parameter plane are found from the simulations and shown to agree with the regions predicted theoretically. The results are consistent with available experimental data.

PACS numbers: 52.35.Mw, 52.35.Nx

The significant mechanisms in the different processes for double-layer formation are still unclear. Experiments in a Q machine[1] and in a differentially pumped triple-plasma machine[2] have shown that an applied step voltage is supported either by a cathode sheath or by a potential drop extending over many hundreds of Debye lengths in the plasma. These two states exist for several electron transit times, and a double layer forms on the time scale of the subsequent ion motion. In the initial state the density in the triple-plasma machine varied axially, forming an ion-density cavity, in contrast to the axially homogeneous plasma column in the Q machine. It has been shown by numerical simulations with periodic boundary conditions that plasma density cavities generated by a low-frequency wave can support applied potential drops,[3] and these results were used to interpret electric fields observed above the aurora.[4] Ion-density cavities can also strongly modify the nonlinear evolution of plasma oscillations.[5]

In this paper we present a new analytical model giving explicitly the potential profiles over an ion-density cavity in a diode when the cavity width is much larger than the Debye length. Numerical simulations are also presented which, in contrast to the periodic boundary conditions used elsewhere,[3] have "electron-rich" boundary conditions similar to those in the experiments and accordingly allow the number density N_0 of the injected electrons to be higher than the particle number density N_1 in the initial plasma. The shape of the cavity potential profiles is found to be independent of N_0, which only controls the sheath potential drops. States similar to the two different experimental states have already been observed in separate numerical simulations.[3,6] As a new simulation result we observe the transition between these two states and find the existence regions of the states in the appropriate parameter plane. These regions are also found to agree with those obtained from the analytical model proposed.

A one-dimensional "particle-in-cell" code[7] is used. The time step was $(2\omega_{pe})^{-1}$ and the grid size $\lambda_D/4$. Here $\lambda_D=(k_BT_e/m_e)^{1/2}/\omega_{pe}$ and $\omega_{pe}=(N_1e^2/m_e\varepsilon_0)^{1/2}$. The maximum density was 10^3 particles per Debye length. The electric potential $\phi(x)$ and the applied potential drop ϕ_a are measured in units of k_BT_e/e. Ions and electrons are injected symmetrically at the two boundaries with half-Maxwellian velocity distributions with a density N_0. We use the natural ion-to-electron mass ratio (argon), and the simulations cover a few electron transit times (about $300\omega_{pe}^{-1}$). For such short simulation times the velocity distribution of the ions present initially is of little significance, as was shown by several runs with different velocity distributions. Here we assume that the initial velocity distributions are Maxwellian with the same temperatures as those of the particles injected. The initial ion-density distribution $n_{ip}(x)$ is, however, of great importance since it may give rise to an electric field controlling the electron motion. We consider a diode in the region $0<x<L$. As a suitable test profile we use

$$n_{ip}(x)=N_1-\Delta N\cos^2\{\pi(x-\tfrac{1}{2}L)/L\}. \quad (1)$$

The profile describes a symmetric cavity with a density N_1 at the boundaries and with a relative depth of $\Delta N/N_1$. The initial potential profile was obtained by a presimulation of a short-circuited diode ($\phi_a=0$) during $0<t<t_1$. For $t=0$ we put $n_e(x)=n_i(x)$ so that the electric potential vanished everywhere. After twenty or thirty plasma periods a self-consistent potential profile was obtained with sheath potential drops approximately given by the Boltzmann relation, $(k_BT_e/e)\ln(2N_0/N_1)$, as shown in Fig. 1(a) for $t=19$. The density at each boundary is $2N_0$ in this initial, symmetric state. In the experimental plasmas there are also ion-density drops in the sheaths. We have tested the significance of such drops by adding ion-density profiles to (1) with a sharp density increase over typically five Debye lengths where the ion number density increased from N_1 to the value $2N_0$ at the boundaries. No significant changes of the potential profiles in the plasma region were observed.

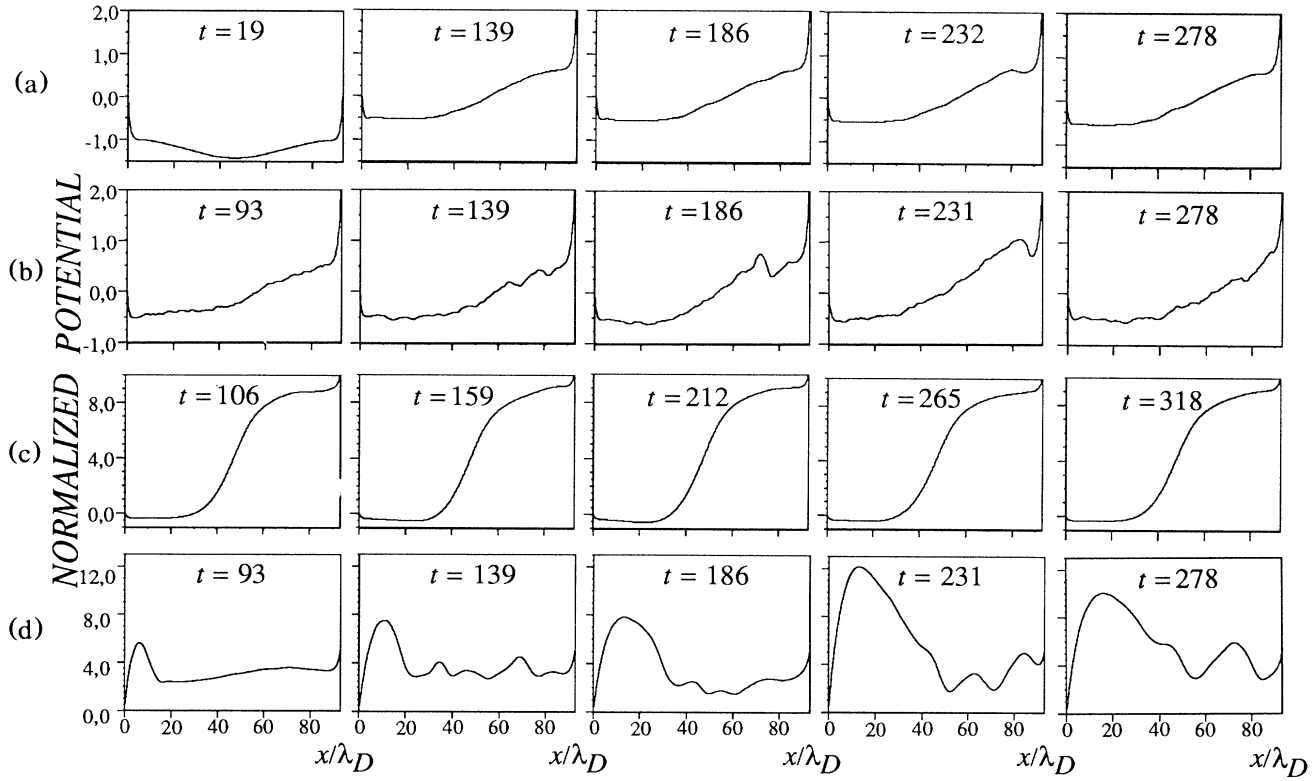

FIG. 1. Simulated potential profiles at times given in ω_{pe}^{-1}. The zero level is at the left boundary. A voltage drop ϕ_a was applied between the boundaries at $t \approx 25$. (a) The initial profile ($t=19$) and profiles at later times which are averaged over $50\omega_{pe}^{-1}$ ($\phi_a=2$, $\Delta N/N_1=0.3$, $N_0/N_1=1.36$). (b) Instantaneous profiles for the same parameters. (c) The steepening of the profile for large cavity depths ($\phi_a=10$, $\Delta N/N_1=0.83$, $N_0/N_1=1.04$). In (d), ϕ_a exceeds the critical voltage drop shown in Fig. 2 ($\phi_a=5$, $\Delta N/N_1=0.3$, $N_0/N_1=1.36$). The profiles in (c) and (d) are averages over $10\omega_{pe}^{-1}$.

For $t=t_1$ a potential drop was applied so that a linear potential variation was superimposed on the initial profile. In Figs. 1(a) and 1(b) examples are given of the cavity potential profiles obtained. These remained approximately stationary during the whole simulation time after an initial transient lasting for about a transit time. Figure 1(c) shows that the cavity potential profile steepens and resembles a double layer for large cavity depths. When ϕ_a exceeds a certain critical value, $\phi_a=\phi_{a1}$, which was found to be a function of only $N_0/(N_1-\Delta N)$, the cavity potential drop disappears, and most of the voltage is concentrated in a cathode sheath [Fig. 1(d)]. As shown in Fig. 2, the critical voltage drops inferred from the simulations agree very well with the theoretical values of ϕ_{a1} derived below as the maximum values of ϕ_a that are consistent with a potential minimum within the diode.

The evaluation of the cavity potential profiles presented below is based on the following assumptions. The electron distribution function is given by the steady-state solution of the Vlasov equation on the assumption that ϕ decreases monotonically from the value ϕ_c at $x=0$ to a minimum at $x=x_0$, where we put $\phi=0$ (in the diagrams $\phi-\phi_c$ has been plotted), and then increases monotonically to $\phi_c+\phi_a$ at $x=L$. The ion motion is neglected during the first few electron transit times, so that the ion density is given by (1). The quasineutrality condition is then used to calculate $\phi(x)$. The electron distribution func-

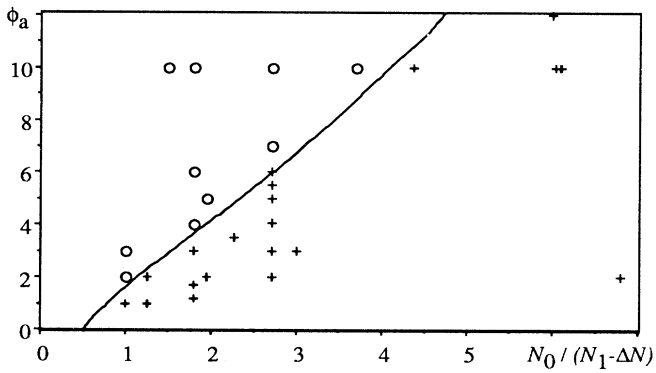

FIG. 2. The circles denote simulations giving voltage drops concentrated in a cathode sheath and the crosses those giving cavity potential drops and potential profiles with a minimum. The solid line gives the maximum value of the applied voltage consistent with the existence of a potential minimum according to (6).

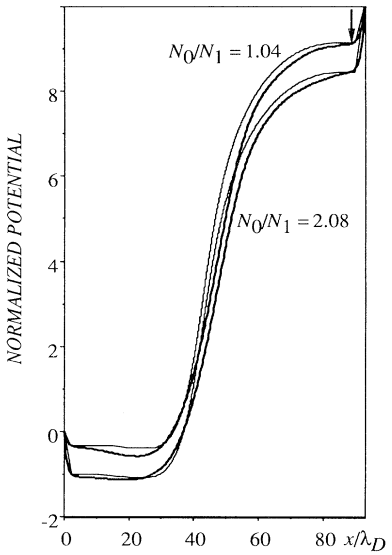

FIG. 3. Profiles obtained for two different values of N_0/N_1 showing that only the sheath potential drops change, whereas the shape of the cavity potential profile remains the same ($\phi_a = 10$, $\Delta N/N_1 = 0.83$; thin lines, theory; heavy lines, simulations). In the theoretical curves the sheath potential drops are indicated by straight lines since (7) determines $\phi(x)$ only in the plasma region. Figure 4 shows the velocity distribution at the point marked by the arrow.

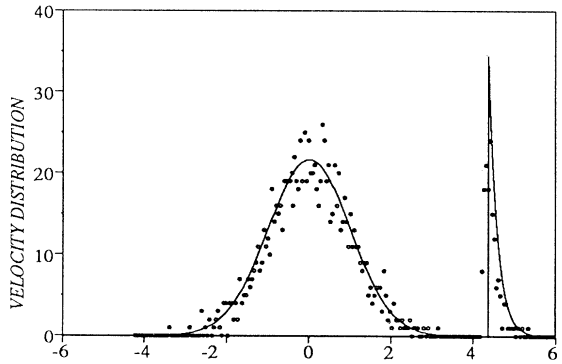

FIG. 4. Comparison between the theoretical electron velocity distribution (solid lines) and the simulated one (circles). The parameters are the same as in Fig. 3 ($N_0/N_1 = 1.04$), and the position is $x = 87\lambda_D$. The velocity is given in units of $v_t = (k_B T_e/m_e)^{1/2}$. The sampled velocity interval is $0.05 v_t$ and the space interval $2\lambda_D$.

tion f becomes

$$f = N_0 \exp(-\phi_a - \phi_c + \phi) F(v), \quad -\infty < v < v_1\sqrt{\phi}, \tag{2}$$

$$f = N_0 \exp(-\phi_c + \phi) F(v), \quad v_1\sqrt{\phi} < v < \infty. \tag{3}$$

Here $v_1 = \mathrm{sgn}(x - x_0)(2k_B T_e/m_e)^{1/2}$, and $F(v)$ is a Maxwellian velocity distribution, normalized to unity when integrated over the interval $0 < v < \infty$. Because of the asymmetry introduced by the applied voltage ϕ_a, the electron distribution function f is discontinuous for $v = v_1\sqrt{\phi}$ which separates the two different contributions to f from each of the boundaries. By integrating (2) and (3) and rearranging the terms the electron number density is obtained as

$$n(\phi) = n_0 \exp(\phi - \phi_c)\{\coth(\phi_a/2) \pm \mathrm{erf}\sqrt{\phi}\}, \tag{4}$$

where $n_0 = N_0\{1 - \exp(-\phi_a)\}$. The upper sign gives the density $n_1(\phi)$ for $x < x_0$ and the lower sign $n_2(\phi)$ for $x > x_0$. The error function is normalized to unity for large values of its argument. $n_1(\phi)$ increases monotonically. As can be shown by differentiation, $n_2(\phi)$ decreases from $n(0)$ to a minimum for $\phi = \phi_m$ and increases monotonically for $\phi > \phi_m$. The condition for a density minimum for $\phi = \phi_m$ is given by

$$\coth(\phi_a/2) = \mathrm{erf}\phi_m^{1/2} + \exp(-\phi_m)/(\pi\phi_m)^{1/2}, \tag{5}$$

which determines ϕ_m as a monotonically increasing function of ϕ_a. Equation (5) is used to eliminate $\coth(\phi_a/2)$ in (4). Then, as a first condition for quasineutrality, we require neutrality at the density minimum $\phi = \phi_m$, where the ion number density is $N_1 - \Delta N$ from (1). This gives

$$(N_1 - \Delta N) = n_0 \exp(-\phi_c)/(\pi\phi_m)^{1/2}, \tag{6}$$

which determines ϕ_c as a function of ϕ_a. It is convenient to normalize n_1 and n_2 to the minimum density given by the right-hand side of (6). Quasineutrality at any point in the plasma region then requires

$$\frac{n_{ip}(x)}{N_1 - \Delta N} = \exp(\phi - \phi_m) + (\pi\phi_m)^{1/2} \exp(\phi)(\mathrm{erf}\phi_m^{1/2} \pm \mathrm{erf}\phi^{1/2}), \tag{7}$$

where $n_{ip}(x)$ is given by (1). $\phi(x)$ can now be evaluated for any given value of $\Delta N/N_1$ by specifying a value of ϕ_m corresponding to any desired value of ϕ_a. Equation (7) also gives the potential levels ϕ_1 and ϕ_2 at the plasma-sheath boundaries, and the sheath potential drops, $\phi_c - \phi_1$ and $\phi_c + \phi_a - \phi_2$, can be evaluated by determining ϕ_c from (6). A number of comparisons between profiles obtained from the theory and the simulations show a very good agreement also in the case when the cavity potential profile is steep ($\Delta N/N_1 = 0.83$) so that it resembles a double layer as shown in Fig. 3.

Equation (6) defines ϕ_c as a monotonically decreasing function of ϕ_a for any fixed value of $N_0/(N_1 - \Delta N)$. For $\phi_a = 0$, ϕ_c is given by the Boltzmann relation, $\ln(2N_0/N_1)$, and the potential minimum coincides with the density minimum. When ϕ_a is increased, the potential minimum moves towards the left boundary and ϕ_c decreases. Finally, ϕ_c vanishes for a value $\phi_a = \phi_{a1}$, and then the potential minimum is at the left boundary. ϕ_{a1}, which is shown in Fig. 2, is the largest possible value of ϕ_a that is consistent with a potential minimum in the diode. When $\Delta N/N_1 \to 1$, (6) predicts arbitrary large values of ϕ_{a1}. Further investigations including the Pois-

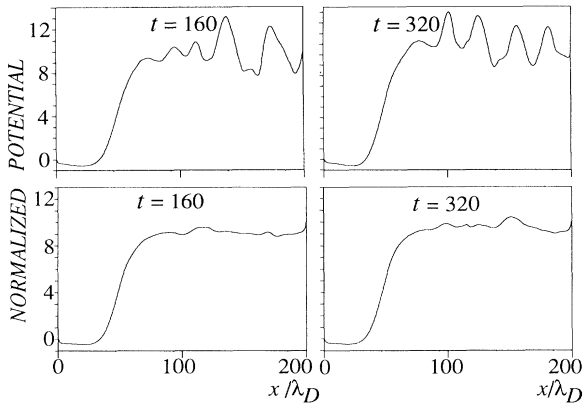

FIG. 5. The parameters are the same as in Fig. 4 except that an interaction region of $100\lambda_D$ with a constant ion number density N_1 is added on the high potential side of the cavity. The upper diagrams show instantaneous profiles and the lower ones, averages over $10\omega_{pe}^{-1}$. The time-averaged cavity potential drop remains the same as for the shorter system (Fig. 3). The beam population is strongly dispersed at $x = 200\lambda_D$.

son equation are necessary to explore this limiting case.

The electron distribution functions simulated show a good agreement with those given by (2) and (3) for the diode lengths considered so far. However, as shown in Fig. 4, a slight discrepancy between the beam distributions can be observed close to the right boundary where the distribution is unstable. To get the first evidence of modifications of the cavity potential profile due to beam-plasma interaction, a longer system was considered. The initial ion number density n_{ip} was given by (1) in the interval $0 < x < 100\lambda_D$ and by a constant value, $n_{ip} = N_1$, in $100\lambda_D < x < 200\lambda_D$, thus allowing an interaction region of $100\lambda_D$. Propagating fluctuations now develop, and the beam population is strongly dispersed at $x = 200\lambda_D$. The relevant result for the work presented here is that this interaction does not modify the time-averaged cavity potential profile significantly, as shown in Fig. 5.

This work has been financed by the Swedish Natural Science Research Council. We wish to thank Dr. P. Gray for providing us with suitable numerical codes and Dr. I. Axnäs, Dr. N. Brenning, Dr. A. Peratt, Dr. N. Singh, Dr. M. A. Raadu, and Professor C.-G. Fälthammar for useful discussions.

[1]S. Iizuka *et al.*, Phys. Rev. Lett. **48**, 145 (1982); J. Phys. Soc. Jpn. **54**, 2516 (1985).

[2]M. Bohm and S. Torvén, in *Proceedings of the Eighteenth International Conference on Phenomena in Ionized Gases. Contributed Papers,* edited by W. T. Williams (Institute of Physics, Bristol, 1987), Vol. 2, p. 318.

[3]H. L. Rowland and P. J. Palmadesso, J. Geophys. Res. **92**, 299 (1987).

[4]M. Temerin, K. Cerny, W. Lotko, and F. S. Mozer, Phys. Rev. Lett. **48**, 1175 (1982); R. Boström *et al.*, Phys. Rev. Lett. **61**, 82 (1988).

[5]E. Infeld, G. Rowlands, and S. Torvén, Phys. Rev. Lett. **62**, 2269 (1989).

[6]N. Singh, Plasma Phys. **24**, 639 (1982).

[7]W. S. Lawson, J. Comput. Phys. **80**, 253 (1989).